ACTA
PROTOZOOLOGICA

Acta Protozool. (2025) 64: 21–35
www.ejournals.eu/Acta-Protozoologica
doi:10.4467/16890027AP.25.003.21935

A gruesome garden of earthly delights: Cadaver decomposition fosters the development of specific eukaryotic microbial biodiversity

Christophe V.W. SEPPEY[1,2], Monika K. RECZUGA[2,3,4], Bertrand FOURNIER[1], Enrique LARA[2,5], Guillaume LENTENDU[2], Matthieu MULOT[1], David SINGER[6], Ildikò SZELECZ[2,7], and Edward A.D. MITCHELL[2]

[1] **Institute of Environmental Science and Geography, University of Potsdam, Karl-Liebknecht-Strasse 24–25, 14476 Potsdam-Golm, Germany**
[2] **Laboratory of Soil Biodiversity, University of Neuchâtel, Rue Emile-Argand 11, 2000 Neuchâtel, Switzerland**
[3] **Laboratory of Wetland Ecology and Monitoring, Faculty of Geographical and Geological Sciences, Adam Mickiewicz University, Dzięgielowa 27, 61-680 Poznań, Poland**
[4] **Institute of Environmental Biology, Faculty of Biology, Adam Mickiewicz University, Umultowska 89, 61-614 Poznań, Poland**
[5] **Real Jardín Botánico, CSIC, Plaza de Murillo 2, E-28014 Madrid, Spain**
[6] **Changins, HES-SO University of Applied Sciences and Arts Western Switzerland, Route de Duillier 52, 1260 Nyon, Switzerland**
[7] **Institute of Forensic Medicine, Goethe University, Kennedyallee 104, D-60596 Frankfurt, Germany**

Abstract. Decomposing cadavers have a strong impact on the soil environment and the biodiversity of soil organisms. However, exploring these patterns in different natural settings, and beyond the first few weeks post-mortem remains a research priority. The response of soil communities to decomposing cadavers could be used for estimating the post-mortem interval (PMI), for which current models are lacking beyond 4–6 weeks.

We conducted a 35-month field experiment using pig carcasses (*Sus scrofa* Linnaeus) in a deciduous forest in Switzerland to characterise the impact of decomposing cadavers on the diversity and community composition of soil micro-eukaryotes by high throughput sequencing of soil environmental DNA.

The diversity of soil microbial eukaryotes strongly declined under decomposing cadavers. Several taxa which were rare in control soils became more abundant in cadaver-impacted soils. The clear temporal succession and turnover in soil microbial eukaryote diversity and community structure underneath cadavers offers potential for inferring the PMI.

The diversity of soil micro-eukaryotes remains poorly documented, especially in under-studied habitats such as cadaver-impacted soils. Characterising this "rare biosphere" diversity will help better understand cadaver impacts on terrestrial ecosystems and is necessary to develop new PMI tools.

Keywords: disturbance ecology, forensic ecology, soil biodiversity, protist, metabarcoding, post-mortem interval

Address for correspondence: Edward A.D. Mitchell, Emile-Argand 11, CH-2000 Neuchâtel, Switzerland; E-mail: edward.mitchell@unine.ch

INTRODUCTION

Carcass decomposition represents a strong, but spatially and temporarily limited, natural perturbation that contributes to the heterogeneity and functioning of all ecosystems through its role in the redistribution of nutrients and energy within and among ecosystems (Carter et al. 2007; Fiedler et al. 2023). The ephemeral pulse of matter input released by a cadaver modifies nutrient pools and fluxes in the soil underneath (Benninger et al. 2008; Aitkenhead-Peterson et al. 2015; Fancher et al. 2017), to which the soil microbiome responds (Stokes et al. 2009; Cobaugh et al. 2015; Metcalf et al. 2016; Pawlett et al. 2019, Mason et al. 2023). In return, soil microorganisms contribute to accelerating the decomposition process (Lauber et al. 2014). The biodiversity and bioindication potential of soil microorganisms associated with cadaver decomposition has recently received increasing attention (Finley et al. 2015), and these studies have recently included microbial eukaryotes (Parkinson et al. 2009; Metcalf et al. 2016) that are often not included in studies of soil microbial diversity (Geisen et al. 2018, 2020). Given the immense diversity of soil organisms largely determined by the high diversity of terrestrial ecosystems and soil types (Anthony et al. 2023; Singer et al. 2021) it remains unclear to what extent patterns observed in one region are universal, even when soil micro-eukaryotic diversity is analysed at relatively coarse taxonomic resolution using metabarcoding approaches.

Decomposing carcasses release large amounts of carbon and nutrients, especially nitrogen and phosphorus, to the surrounding environment (Carter et al. 2007; Benninger et al. 2008; Barton et al. 2013). The presence of a decomposing carcass also changes the soil microclimate (Carter et al. 2010). Annual mammal carcass inputs can be substantial, e.g. 557 kg of animal weight per square kilometre in a Neotropical rainforest (Houston 1985) and 5 000 kg of bison carcass in 988 ha of the North American tallgrass prairie (Carter et al. 2007). This organic matter input from animal carcasses is highly patchy and may contribute disproportionately to the overall transfer of nutrients and energy within and among terrestrial ecosystems compared with plant litter (Barton et al. 2013).

This transient nutrient input creates a spatial and temporal hotspot of biological activity and is known as the "cadaver decomposition island" (CDI). CDIs are characterised by major changes in the biomass, community composition and activity of different groups of soil organisms, including increased microbial biomass and activity, and changes in bacterial communities, and nematode abundance (Carter et al. 2007; Howard et al. 2010; Brenton et al. 2016; Szelecz et al. 2016; Wang et al. 2021). CDIs are hotspots of energy and nutrient exchange and host specialised communities that contribute to the biodiversity and functioning of terrestrial ecosystems (Carter et al. 2007; Barton et al. 2013). For many arthropods, carcasses constitute a vital food source at certain stages of their development, for others it is a habitat where interactions with other species occur (Hanski 1987). Carcass-impacted soils follow an ecological succession associated with the altered soil chemical environment, as shown for Bacteria and Fungi (Moreno et al. 2011; Carter et al. 2015; Metcalf et al. 2016; Adserias-Garriga, et al. 2017; Fu et al. 2019; Wang et al. 2021;), euglyphid testate amoebae (Szelecz et al. 2014; Seppey et al. 2016), nematodes (Szelecz et al. 2016), and a combination of protists and invertebrates (Forger et al. 2019). Microeukaryotes such as phagotrophic protists (protozoa) and nematodes contribute to C mineralisation and nutrient cycling directly through consumption of various microbial groups (Bouwman and Zwart 1994; Schroter et al. 2003; Aoki et al. 2007; Wilkinson and Mitchell 2010). While the environmental DNA (eDNA) high throughput sequencing (HTS) survey of Seppey et al. (2016) revealed an overall negative impact of cadaver decomposition on the diversity of soil Euglyphid testate amoeba taxa, two phylotypes phylogenetically distant from other taxa in the Genbank DNA database responded positively to carcass impacts for a certain time interval (one month to one year), thus illustrating both the potential of soil eDNA metabarcoding for detecting unknown organisms and the role of carcasses in creating suitable conditions for otherwise rare soil organisms. Most previous studies on cadaver impact on soil organisms were limited in time (4 months at most) or lacked negative controls (Metcalf et al. 2016; Mason et al. 2023; Wang et al. 2021; Parkinson et al. 2009). The impact of decomposing carcasses on most soil microeukaryotic organisms, including most bacterivorous, saprotrophic, and parasitic protists over a longer period therefore remains to be documented.

Knowing how soil communities respond to decomposing cadavers is a prerequisite to developing new tools to estimate the post-mortem interval (PMI) which is a crucial question in forensic investigations when a human cadaver is found (Tibbett and Carter 2009).

Existing PMI tools include legal medical observation of the cadaver itself (rigidity, temperature etc.) and forensic entomology (Turchetto et al. 2001; Amendt et al. 2004; Lefebvre and Gaudry 2009; García-Rojo et al. 2013). However, these tools are only useful in the first hours or days for legal medicine (Szelecz et al. 2014) and for forensic entomology up to approximately 4–6 weeks (Amendt et al. 2004; Anderson 2010; Daria et al. 2011; Szelecz et al. 2014). New tools are needed to estimate longer PMIs and high throughput sequencing of soil eDNA is a promising option (Finley et al. 2015; Metcalf et al. 2016; Mason et al. 2023). Soil abiotic characteristics and soil organisms are prime candidates for developing such a tool as they include a vast array of indicators with different dynamics from fast (e.g., Bacteria, labile chemical compounds) to slower (e.g. invertebrates) (Carter and Tibbett 2003; Braig and Perotti 2009; Dekeirsschieter et al. 2009; Parkinson et al. 2009; Metcalf et al. 2016; Szelecz et al. 2018).

Here, we set out to characterise the diversity of soil micro-eukaryotic communities underneath decomposing cadavers and to assess the response of soil micro-eukaryotic taxa and communities to cadaver-induced disturbance. Specifically, we asked the following questions: (i) Is there a temporal succession in micro-eukaryotic diversity and community structure in cadaver-impacted soils? (ii) Are there taxa specific to cadaver-impacted soils and of different decomposition stages or time steps? (iii) If so, are these taxa present before the start of the decomposition process? (iv) Do taxa specific to cadaver-impacted and to control soils differ taxonomically and ecologically and to the degree to which they are known? Answering these questions will help better document a still poorly explored field of unknown diversity.

MATERIALS AND METHODS

Field experiment

The experiment was conducted in a mixed beech and oak forest near Neuchâtel, Switzerland, (47°00'11.90–12.26" N / 6°56'6.45–8.05" E, elevation 478 m), in a fenced area of approximately 6400 m^2. Within the area, three blocks of approximately 25 m^2 were selected (15–34 m apart), labelled 1–3, each with three plots (90 cm × 100 cm) corresponding to one of three treatments: control (coded C), fake carcass (bags filled with soil and covered with a cotton cloth to investigate microclimatic effects without cadaveric fluids, coded F) and pig carcasses (*Sus scrofa* Linnaeus, coded P). The plots were at least four metres apart from one another. The weight of the fake carcasses corresponded to the initial weight of the pig carcasses (i.e. 20 kg, ± 1 kg). As the weight of the pig carcasses decreased through decomposition, a corresponding amount of soil was gradually removed from the fake pig carcass at each sampling day to mimic the weight loss. The choice of pigs (*Sus scrofa* Linnaeus) as research animals was motivated by their common use as models in forensic experiments (Stokes et al. 2013; Belk et al. 2018).

The three pigs were all female, killed by captive bolt stunning and instantly transported and placed on the plots. To enable sampling beneath the carcasses and to avoid disturbance by large scavengers, each carcass was placed in a metal wire cage. The area covered by the cages was marked with a stick in each corner to allow for a proper placement of the cages after sampling. The cages were lifted during sampling and placed back in the exact same position after sampling (Szelecz et al. 2014).

Sampling and chemical analyses

The soil beneath the carcasses and in the other two treatments was sampled immediately before the placement of the carcasses (D0), and after 8 (D8), 15 (D15), 22 (D22), 33 (D33), 64 (D64), 309 (D309) and 1051 (D1051) days from the start of the experiment. The first sampling took place on August 5th, 2009 (before the fake and pig carcasses were placed). For the initial sampling, the soil collected from the nine individual plots was pooled within each of the three blocks to obtain a composite sample for the initial conditions per block. Subsequent samples were then collected for the nine plots separately (no composite sample was made). Soil (ca. 25 g) was collected to a depth of 10 cm in each plot and immediately transported to the laboratory. The samples for DNA extraction were stored at –80°C. To measure total organic carbon and total nitrogen, ca. 3 g of each sample was dried (40°C, 12 hours), ground to powder and analysed using combustion infrared spectroscopy (CHNEA1108-Elemental analyser, Carlo Erba Instrument) after carbonate removal with HCl (Seppey et al. 2016). In detail, carbonate was removed using acid fumigation method: soil samples were weighed in Ag-foil capsules, placed in order on a microtiter plate, saturated with water and put in a desiccator with a beaker with 12M HCl for ca. 7 h (Seppey et al. 2016). For detailed information on total carbon and nitrogen see Seppey et al. (2016).

DNA extraction, PCR amplification and high-throughput sequencing

DNA was extracted using the MoBio Power Soil DNA isolation kit (Carlsbad, CA USA) according to the instructions provided by the manufacturer. PCR amplification of gene sequence encoding the 18S rRNA V9 region was carried out with eukaryotic-specific primers 1380F (CCCTGCCHTTTGTACACAC) and 1510R (CCTTCYGCAGGTTCACCTAC) (Seppey et al. 2016). PCR was conducted according to the following conditions: denaturation at 94°C for 3 min, 30 cycles at 94°C for 30 sec, 57°C for 60 sec and 72°C for 90 sec and final extension at 72°C for 10 min (Seppey et al. 2016). The PCR mixture was constituted of 1 ng of environmental DNA, 6 µL of 10x PCR buffer, 0.6 µl of each primer, 0.6 µl of dNTP 400 µM (Promega) and 0.2 µl of 0.05 U/µl Go Taq (Promega). The purification step was done using a PCR Purification Kit (Qiagen, Hilden, Germany) followed by DNA library preparation with NEBNext DNA Sample Prep Master Mix Set 1 (New England Biolabs, http://www.neb.com/nebecomm/ManualFiles/manualE6040.pdf) excluding the size selection step. Paired end sequencing was per-

formed by the Genomics Core Facility at Brown University (Providence, USA) with an Illumina HiSeq 2000 sequencer and provided and overall 47,156,126 sequences of 2*75 bp. The raw sequences are available on ENA-EMBL under the project PRJEB25144. Further details can be found in Seppey et al. (2016), in which a subset of the data (i.e. euglyphid testate amoebae) was analysed.

Sequence analyses

The computational pipeline used to analyse the reads is available at GitHub (https://github.com/lentendu/DeltaMP ; v0.4) and includes the following steps: trimming of the tagged primer sequences, merging, quality check, clustering, chimaera sequences removal, taxonomic assignation. Primers were removed from 5'-end of reads using cutadapt v1.18 (Martin 2011) allowing until 6 mismatches. Reads were pair-end assembled using the "simple_bayesian" algorithm of pandaseq v. 2.11 (Masella et al. 2012). Reads were further filtered out if the average phred score was below 20 or the length was below 90 nt or above 200 nt using MOTHUR v.1.42.0 (Schloss et al. 2009). Sequence clustering was then done using Swarm v.2.2.2 (Mahé et al. 2015) with the fastidious option, and OTUs were checked for chimaera using the UCHIME algorithm as implemented in vsearch v.2.9.1 (Rognes et al. 2016). Non-chimeric OTUs were taxonomically assigned by aligning the most abundant sequence of each OTU against the PR^2 database v.4.14.0 (Guillou et al. 2013, https://github.com/pr2database/pr2database) using the global pairwise alignment method of vsearch with default parameters (i.e. without end-gap allowed). For that, the PR^2 reference sequences were first trimmed according to the amplified fragment using cutadapt. Protist function was inferred from taxonomy following Lentendu et al. (2025).

Statistical analyses

The community matrix was first pre-processed by removing the Embryophyceae (i.e. plants) and Metazoa, with exception of Nematoda which were proven useful in forensic sciences (Szelecz et al. 2016). The OTUs with a percentage of identity (PID) below 60% with the PR^2 database were also removed as putative prokaryotes. Spurious taxonomic assignments were also corrected by lowering the taxonomic resolution after pairwise alignment (BLASTn, Camacho et al. 2009) on the GenBank database. As such, OTUs assigned to Syndiniales were considered as unknown Alveolata, and Radiolaria and Haptophyta were considered as unknown Eukaryotes. We also discarded OTUs with low information, namely having only one non-zero value or sharing a ratio between the two most common values above 95/5 and several unique values below 8 (nearZeroVar pgk caret: Kuhn 2020). From this abundance matrix, we calculated the relative abundance of each OTUs in each sample (comm_relabu) and the centred log ratios after replacing the null values by geometric multiplicative replacement (cmultRepl pkg zCompositions: Palarea-Albaladejo and Martin-Fernandez 2015).

OTUs characteristic of carcass presence (CPI = carcass presence indicator) or absence (CAI = carcass absence indicator, including control and fake pig treatments) at any time periods between 8 and 1051 days (PMI) were then identified by calculating indicator values following the method of De Cáceres and Legendre (2009) using the function multipatt of the R package indicspecies v. 1.7.12. An indicator value was considered significant if the probability of having a higher value by chance was below 0.01.

We then assessed microbial eukaryote alpha diversity using the richness, Shannon index, the residual of a linear model between the richness and the number of sequences, and the Pielou's evenness. To assess the changes in community structure (beta diversity) over time and among treatments, we calculated a non-metric multidimensional scaling (NMDS) of the community relative abundance data. We then tested the correlation between the community structure and the treatments, PMI, carbon, and nitrogen by permutation test (999 permutations).

We calculated for each time point the Accumulated Degree Days (ADD) and compared these values with the PMI. Additive degree days (ADD) were estimated using the nearest meteorological station with the lowest variance in temperature with the study site, as computed using a Swiss wide climatic model (Külling et al. 2024). The meteorological station of Neuchâtel (Switzerland) was chosen with an average of + 1.0°C (+/– 0.08°C) difference during the four years of the experiment (2009–2012). ADD was computed as the cumulative sum of days with an average daily temperature > 0°C at the experimental site (that is > 1°C at the meteorological station of Neuchâtel) from the first day of the experiment, using open Swiss meteorological station data (Swiss Federal Office for Meteorology and Climatology MeteoSwiss).

All statistical analyses were conducted in R v.4.3.0. A compiled version of the full code used for analysis is provided in a repository at https://gitlab.com/cseppey/cadaver_bioindic.

RESULTS

Diversity and structure of the eukaryotic OTU assemblage

The Illumina sequencing generated 41,744,854 raw Eukaryote SSU V9 reads clustered into 264,875 OTUs. After the preprocessing 36,612,273 reads were retained and clustered into 13,869 OTUs. In the non-carcass plots (controls and fake pigs) Fungi accounted for 85.9% of the micro-eukaryotic reads. Among protists, the dominant groups were Rhizaria (3.7%), Alveolata (3.0%) and Stramenopiles (1.1%) (Fig. S1). In the carcass impacted soils, the proportion of fungal sequences was significantly lower (47.1% Wilcoxon test $P < 0.05$), whereas the proportion of protists was higher, with highest contributions of Rhizaria (19.5%), Fonticulidae (10.1%), Alveolata (5.6%) and Excavata (2.7%) and a clear increase in the number of Nematode sequences (7.2%) (Fig. S1).

Decomposition stages and chemical variation along time

The carcasses followed the decomposition stages described in Payne (1965): fresh (D0), bloated (D2, not sampled), active decay (D8–D15), dry (D22–D64) and remains (D309) up to the point when only scattered

bones were left (D1051), a stage we refer to as "dry remains". Over the course of the experiment, the PMI was well correlated to the accumulated degree day (ADD); but ADD at first increased somewhat more than PMI during the first weeks (summer) (Fig. S2). Carcass decomposition caused an increase in total N concentration starting from D8 (0.72% ± 0.15 SE) as compared to the fake carcass and control (0.39% ± 0.05 and 0.51% ± 0.06 SE respectively), reaching the highest value 309 days after the beginning of the experiment (1.17% ± 0.48 SE). Similarly, total C concentration was highest on day 309 (13.9% ± 4.8 SE). The C/N ratio decreased underneath the carcass from D0 (18.0 ± 1.3 SE) to D15 (10.8 ± 0.7 SE) and remained low (ca. 10) until D64, followed by an increase to the level of the control by D1051 (control: 17.0 ± 1.8; fake cadaver: 18.5 ± 1.1; pig: 16.5 ± 0.9) (Fig. S2).

Identification of carcass indicators

In total, 1914 OTUs (i.e. 13.8% of all 13,869 OTUs) were indicators of either carcass absence (CAI, 1628 OTUs, 11.7%) or presence (CPI, 286 OTUs, 2.1%). The sub-group of carcass absence indicators (CAI) were composed of a high percentage of Pezizomycotina (26%), Agaricomycotina (47%) and Mucoromycotina (12%) in addition of some Rhizaria (3%), Alveolata (2%) and Stramenopiles (1%) (Fig.1). Under the pig carcasses most of the indicator OTU reads were assigned to *Fonticula alba* (69%) in addition to parasitic Alveolata (Colpodellidae: 5%) and Amoebozoa (6%). Fungal indicators were less numerous than underneath the cadaver (8% as opposed to 91%) (Fig. 1). The full list of indicators OTUs is given in Table S1.

Changes in protist community alpha diversity

Shannon diversity and OTU richness were influenced by cadaver decomposition (Fig. 2). Shannon diversity decreased sharply after 8 days, associated with the early decomposition phases, and recovered after 1051 days. Overall, micro-eukaryotic Shannon diversity was significantly lower in the carcass samples as compared to both control and fake carcass samples (Kruskal-Wallis test $P < 0.001$). The richness showed a similar pattern with lower values for the carcass from D8 to D309 (Table 1).

Changes in protist community composition

The NMDS ordination (Fig. 3) shows that the carcass treatment communities clearly diverged from the control and fake carcass in the ordination space from D8 until D309 (Table 2, Fig S7). A permutation test showed a significant relationship between the structure of micro-eukaryotic communities and treatment, nitrogen (permutation test, both $p < 0.01$) and carbon ($p < 0.05$).

Soil protist community composition differed among treatments (Fig. S1) as well as over time in cadaver-impacted soils (Fig. S3). The initial communities in cadaver-impacted soils were dominated by Fungi, mostly Agaricomycotina (number 23 in Fig. S3), Pezizomycotina (nr 21) and Mucoromycotina (nr 27). At D8, the proportion of bacterivorous taxa (e.g. *Fonticula alba* -related (nr 34), Cercomonads (nr 40), Nematoda (nr 32), Parabodonida (nr 17) and Lobosea (nr 12–15)) started to increase whereas the proportion of Fungi decreased. The proportion of these bacterivorous taxa stayed high until D64 and started to decrease thereafter (Fig. S3). By D1051 the carcass impacted samples converged back towards the samples of the other two treatments. However, the proportion of consumers remained

Table 1. Difference of micro-eukaryotic OTU richness and Shannon diversity between each combination of control (C), fake (F) and pig (P) treatments for all post-mortem intervals (PMI) and corresponding accumulated degree days (ADD) and average temperature over the corresponding interval.

	PMI [days]	0	8	15	22	33	64	309	1051
	ADD [°C]	0	159	322	466	649	1146	2713	10536
	Average T [°C]	n.a.	19,9	23,3	20,6	16,7	16,0	6,4	10,5
OTU richness	C-F	1	0,46	0,90	0,64	0,74	0,99	0,55	0,90
	C-P	1	0,74	0,17	0,37	0,23	0,09	0,03	0,64
	F-P	1	0,13	0,07	0,07	0,04	0,13	0,30	0,90
Shannon	C-F	1	0,37	0,99	0,99	0,99	0,37	0,99	0,90
	C-P	1	0,90	0,09	0,09	0,09	0,02	0,09	0,90
	F-P	1	0,17	0,13	0,13	0,13	0,37	0,13	1,00

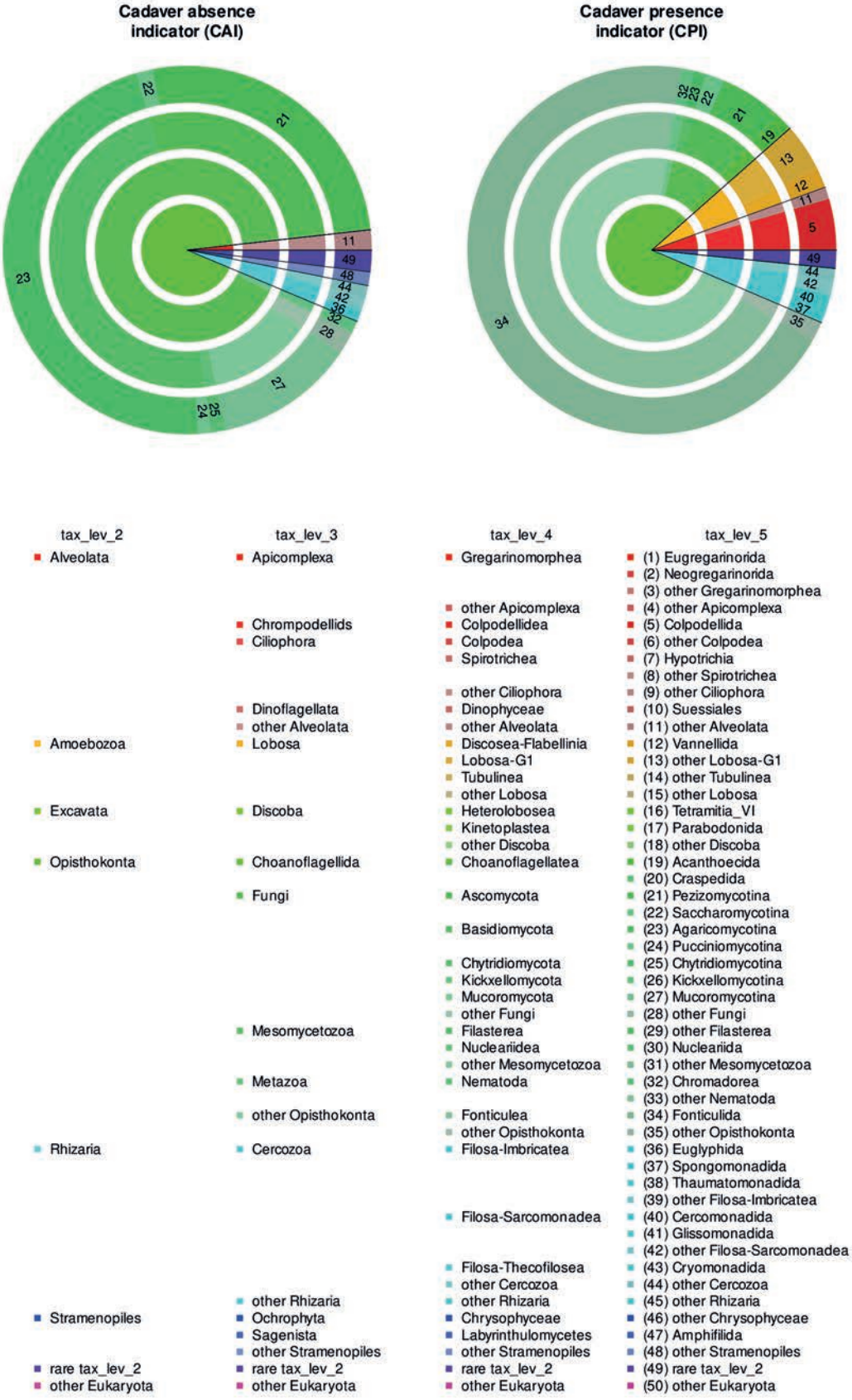

Fig. 1. Taxonomy assigned to the cadaver absence indicators (CAI) and cadaver presence indicator (CPI) OTUs at taxonomic levels 2–5 of PR^2. The proportions are calculated on the average of relative abundances of each OTU across all samples of a given category. Organisms belonging to underrepresented clades at taxonomic level 2 are pooled into the category "rare_tax_lev_2".

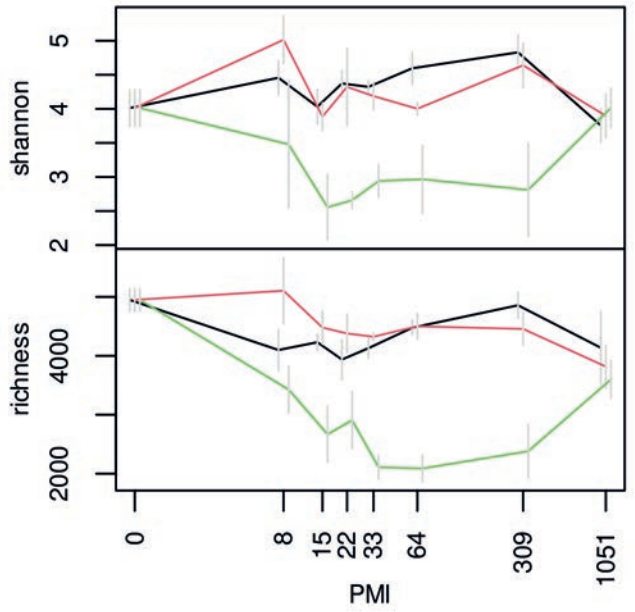

Fig. 2. Diversity indices (Shannon index and OTU richness) calculated from protist OTU communities retrieved from soils impacted by cadaver (green), fake cadaver (red) and control (black) in function of the PMI.

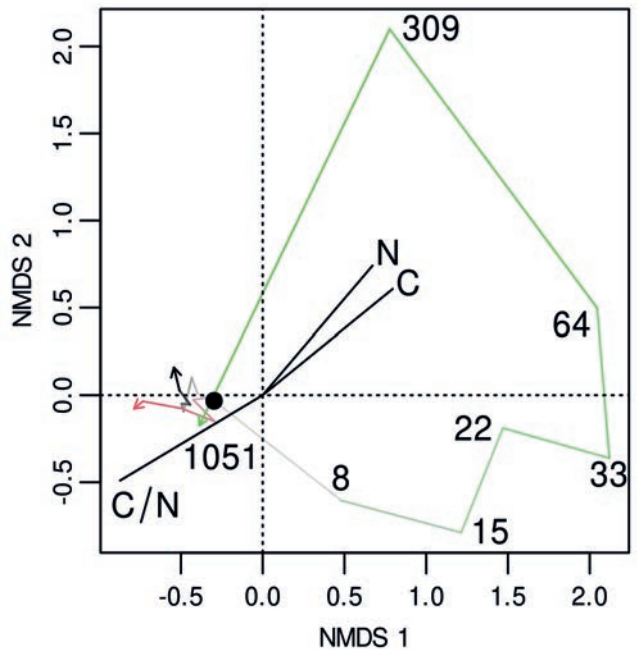

Fig. 3. Non-metric multidimensional scaling (NMDS) calculated on the protist communities retrieved from soil impacted by cadavers (green), fake cadavers (red) and controls (black). The arrows show the change in community through PMI (shown by the number). Stress = 0.17.

Table 2. Significance of the difference in protist beta diversity (difference between cadaver-impacted soil and control) for different postmortem intervals (PMI).

PMI [days]	vs. D0	vs. C
8	0,13	0,15
15	0,06	0,07
22	0,03	0,02
33	0,03	0,01
64	0,03	0,01
309	0,01	0,01
1051	0,16	0,15

higher at the end of the experiment than at the beginning which shows that measurable differences among control and cadaver-impacted soils were still present 1051 days after the beginning of the experiment. Finally, there was a minor but significant difference between the control and fake pig treatments (Fig. S4, permutation test: $p < 0.05$), suggesting a microclimatic effect and a temporal variation on soil micro-eukaryotic communities as well as a significant effect of nitrogen and C/N ratio ($P < 0.01$).

Temporal variation in the relative abundance and composition of cadaver-presence indicators

The relative abundance of the CPIs found in the cadaver plots at D0 was low (0.03%). Thereafter, their relative abundance increased to over 15% during the active decay and most of the dry stage (PMI 8 to 33 days) before decreasing to under 10% in later stages (PMI 64 to 1051 days) (Fig. 4). It is noteworthy that the CAIs were again relatively more abundant than CPIs at the end of the experiment (1051 days postmortem).

The taxonomic composition of the CPIs also changed through the decomposition process (Fig. 5). Noteworthy at first is the high proportion of OTUs closely related to *Fonticula alba*. At D0, Fonticulids constituted 37% of the CPIs; this proportion increased to the near totality of the indicator community (> 96%) during the active decay stage (D8 and D15). The proportion of Fonticulids then decreased through the dry (D22–D64) and remains (D309) stages to 48% ± 16 SD and 10% respectively. Nevertheless, fonticulids were still present in the last part of the decomposition process (D64–D309), due to the presence of OTU X2007,

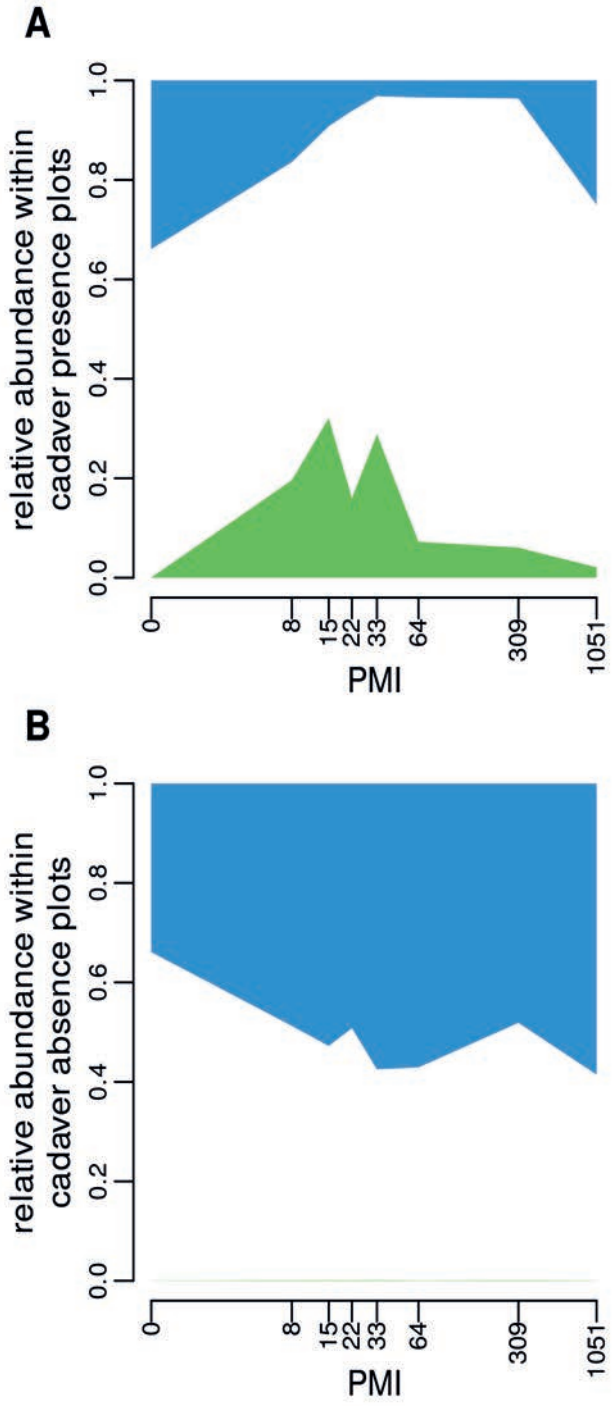

Fig. 4. Temporal trend in the relative abundance of indicator OTUs underneath the cadaver. The OTUs were grouped into cadaver absence indicators (CAI, blue), cadaver presence indicators (CPI, green) and OTUs with no specific indicator value (white).

which was almost absent from the first decomposition stages (Fig. S5, highlighted by a brown box).

Fungi constituted the second largest group of CPIs cumulating at 18% of indicators found in D0. No fungal CPI was present during active decay. However, Ascomycota represented 10 to 22% of the CPIs during the dry stage (D22–D64). The proportion of Fungi (mostly Ascomycota) continued to increase until reaching 27% and 53% of the CPI community in T309 and T1051.

The Alveolata accounted for 17% of the CPIs found at D0 and were dominated by ciliates from the order Colpodea (9%) and the early branching Colpodellida (5%) (Fig. 5). Colpodellida were the only taxon that covered more than 1% of the CPIs during the active decay. During the rest of the experiment, Alveolata continued to constitute a large part of the CPIs, covering from 3% to 17%. Nevertheless, the taxonomic coverage changed through time; OTUs assigned to Colpodellida being present during the dry stage, Eugregarinorida appearing at D64 (4%); and finally Ciliophora (57% and 62% of Alveolata in D309 and D1051).

Rhizarians were dominated by Cercozoa and their proportion among CPIs increased during the dry stage (D22–D64). Most OTUs belonged to Sarcomonadea, a group that remained present through the rest of the decomposition process, particularly in the remains and old remains stages (26% and 70% of Rhizaria in D309 and D051, respectively). In addition, the Imbricatea represented a large proportion of the Rhizaria sequences at the end of the dry, remains and old remains stages (79%, 55%, 30% of Rhizarian CPIs in D64, D309 and D1051 respectively).

Amoebozoa also increased during the dry stage (D22 and D64), particularly during D33 and D64 when this taxon represented 17% and 16% of the CPIs, respectively.

Our results show that about 63% of the carcass indicator OTUs (CPIs) were already present in low relative abundances in the soils before cadaver decomposition occurred. The number (richness) of CPIs found at D0 varied from 147 to 232 (mean=180 ± 30 sd) and increased over time (Spearman correlation: rho = 0.79, p-value < 0.05, Fig. 6). Their proportion at D0 varied from 32 to 41% but did not vary in function of the PMI (Spearman correlation: rho 0.21, p-value > 0.1). Carcass presence indicators were significantly less abundant (lower CLR values, Kruskal-Wallis test $P < 0.001$) in the overall dataset than CAIs, the median CLR values being at 40 and 110 respectively (Fig. S6).

The percentage of identity (PID) of CPIs was lower than for CAIs (median = 95.7% and 96.2%, respectively) (Fig. 7 A). This difference was mostly marked during the dry stage (D22–D64; Fig. 7 B). The proportion of indicators between the seven first taxonomic levels

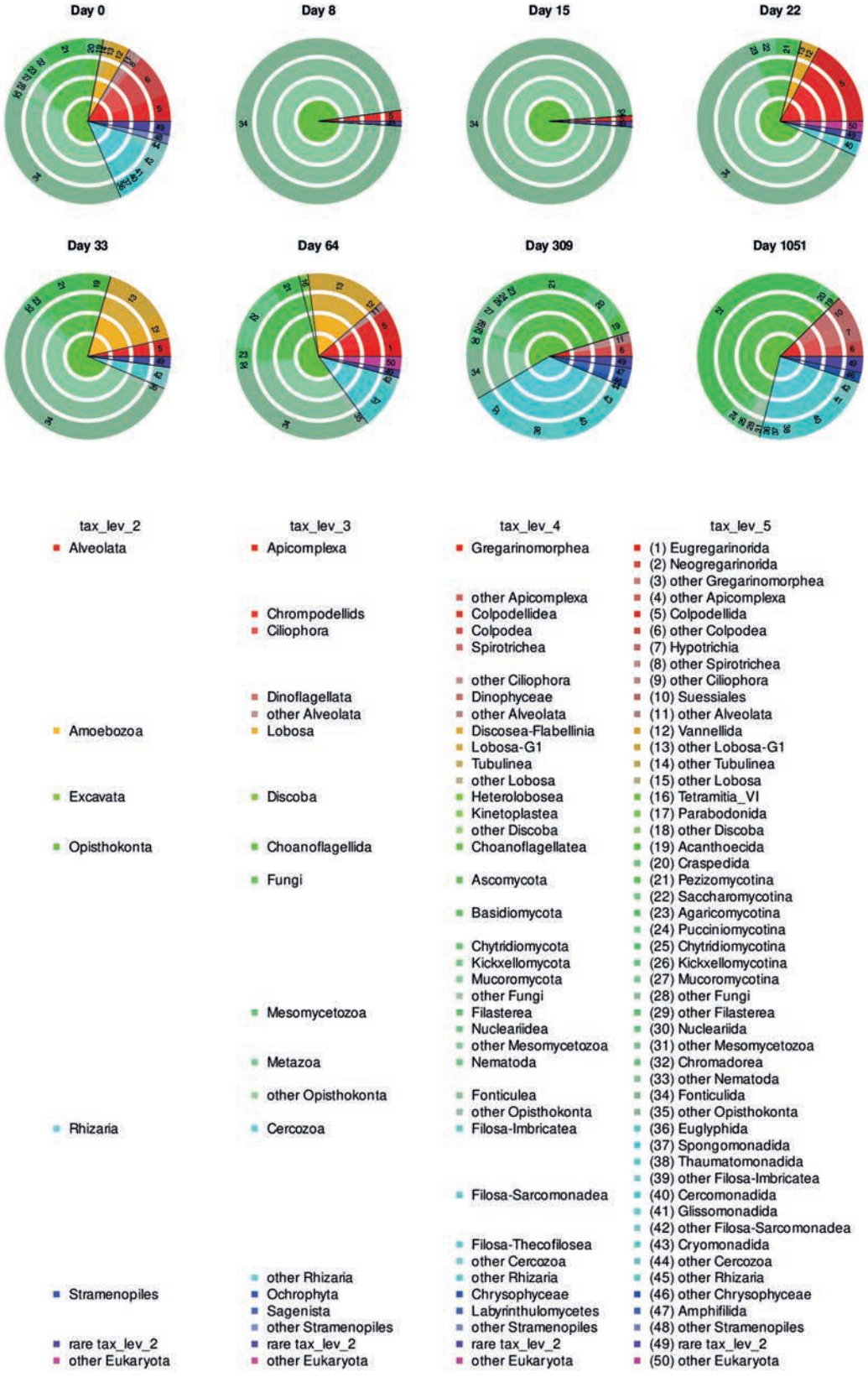

Fig. 5. Taxonomic proportions of carcass indicators through time. The number above the pie charts indicate the PMI. The numbers in each slice indicate the relative abundance of carcass indicators found at each time point. Organisms belonging to underrepresented clades at taxonomic level 2 are pooled into the category "rare_tax_lev_2".

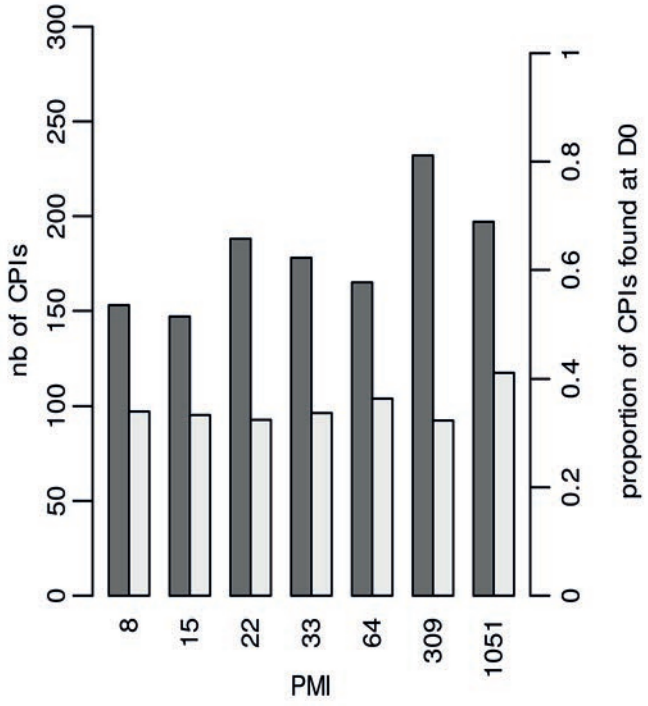

Fig. 6. Dark bars: number of cadaver presence indicator OTUs (CPI) found at each time point (post-mortem interval – PMI). Grey bars: proportion CPI OTUs represented at D0.

(according to PR^2 informal taxonomy) within carcass absence or presence samples was similar (Fig. 7 C). Nevertheless, the percentage of identity of these indicators was significantly lower for the CPIs at high taxonomic resolution (tax_lev_5; Kruskal-Wallis test $P < 0.05$, Fig. 7 B).

DISCUSSION

We characterised the diversity and temporal patterns of soil micro-eukaryotes underneath decomposing pig cadavers in comparison with control and fake pig treatments with the aim of identifying indicators of (1) cadaver presence and (2) of different time steps (post-mortem interval – PMI). Our results clearly confirm that decomposing pig cadavers strongly influences the diversity and community composition of soil micro-eukaryotes. Our results demonstrate that several taxa are specific to either cadaver-impacted soils (cadaver presence indicators, CPI) or non-impacted soils (cadaver absence indicators, CAI) and that CPIs represent an important proportion of the overall micro-eukaryotic community underneath cadavers. In other terms, corpses

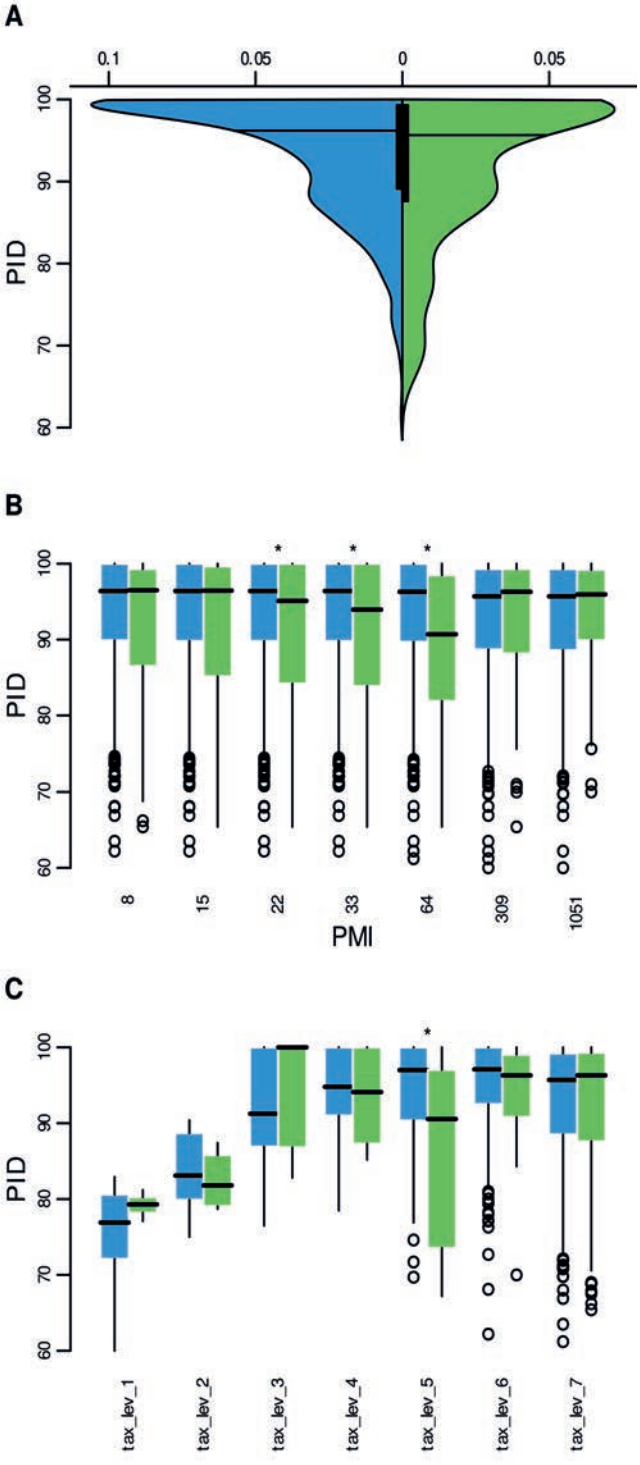

Fig. 7. The density of protist indicator OTUs from carcass absence (CAI, blue) or presence (CPI, green) soils in function of their identity percentage to the PR^2 database (PID). A) black boxes show the 1st and 3rd quartiles of the distribution while the vertical line indicates the median of the distribution. B) and C) respective PID of CAI and CPI OTUs at different taxonomic levels (B) and different post-mortem intervals (PMI).

decomposing in forests host highly specific eukaryotic communities. We also found a clear temporal succession in microbial eukaryote diversity and community structure underneath cadavers, in line with several previous studies (Bergmann et al. 2014; Cobaugh et al. 2015; Metalf et al. 2016; Forger et al. 2019).

The fact that CPIs are taxonomically less known than CAIs suggests that cadavers favour the development of a diversity of lesser known and phylogenetically potentially divergent organisms. Characterising this unknown diversity will contribute to improving the still patchy knowledge on soil biodiversity and may also help better understand the phylogenetic relationships among groups of protists (Lax et al. 2018). Studying the biodiversity of cadaver-impacted soils contributes to alleviating the discrepancy among habitats studied for global biodiversity assessment. This is an example of Racovitzan impediment of knowledge, and hence likely conservation, of the characteristic biodiversity of unexplored environments (Ficetola et al. 2019).

The soil microbial eukaryote micro-fauna specialised to cadaver-impacted soils

About 2.3% of the OTUs underneath pig cadavers were specific to this treatment (CPI) based on indicator value analysis. These taxa were disproportionately abundant, representing up to 32% of the total community 15 days after the beginning of the experiment (Fig. 4). This is particularly striking as these taxa accounted for less than 0.01% of the total relative abundance in the same soils before the beginning of the experiment and in the control plots (Fig. 4B). This confirms that cadaver-impacted soils harbour a specialised micro-eukaryotic diversity composed by taxa adapted to the specific conditions of these habitats.

Temporal succession in micro-eukaryotic communities underneath cadavers

In accordance with our hypotheses, we found clear temporal succession in micro-eukaryotic diversity (Fig. 2) and community structure (Fig. 3) in cadaver-impacted soils. The initial sharp decrease in biodiversity suggests an overall negative impact of decomposing cadavers on micro-eukaryotic communities, as previously observed for different groups of soil micro-organisms (Bergmann et al. 2014). This suggests that many taxa cannot tolerate the initial pulse of organic matter input released by the cadaver and other chemical changes (e.g. pH, phosphorus (Benninger et al. 2008)). This confirms previous results from the same experiment for testate amoebae based on morphological and metabarcoding analyses and extends the conclusion to the entire soil micro-eukaryotic diversity (Szelecz et al. 2014; Seppey et al. 2016). Although this was expected, a striking result was the duration of this effect. After the last sampling (D1051), almost three years after the beginning of the experiment, micro-eukaryotic community composition, but not OTU richness and diversity (Fig. 2), was still clearly different underneath the carcasses as compared to the control plots or initial sampling (Fig. 5, S7). This points towards a slow recovery of microbial eukaryotic communities following the disturbance induced by cadaver decomposition.

Our results confirm the existence of successional stages in soil micro-eukaryotic communities that correspond to cadaver decomposition stages (Fig. 5, S3). We distinguished two time periods with specific trends in soil micro-eukaryotic community taxonomic and functional composition. The period between active decay and dry stage (between D8 and D64) was characterised by an increase in bacterivores such as Chromadorea nematodes, Cercomonadida and Fonticulida, and a decrease in Fungi. Examples of taxa that increased in relative abundance during this period include *Fonticula alba*, different groups within the Cercomonadida (Fig. S3). These taxa likely benefited from the increase in bacterial biomass caused by the nitrogen and carbon-rich cadaveric fluids (Fig. S2) and/or the subsequent reorganisation of the food web. In addition, a stable proportion of the community was assigned to protist parasites from genus *Colpodella* (Mikhailov et al. 2015) during the active and dry stages. Similar organisms have been isolated from pig faeces (Bass et al. 2016), another N-rich environment. Thus, it can be hypothesised that these organisms parasitize bacterivorous micro-eukaryotes that thrive underneath carcasses (Worley et al. 1979).

The period between remains and old remains stage (between D64 and D1051) was characterised by an opposite trend with an increase in Fungi and a decrease in bacterivores. These OTUs most likely did not benefit directly from the release of cadaveric fluids and nutrients in the initial decomposition phase but found favourable conditions during these later stages. During this period, community composition in cadaver-impacted soils progressively became more similar to that of non-impacted soils, without returning to the initial community composition, possibly due to the accumulation of dormant stages of CPIs. The speed of this recovery likely depends on the changes in environmental

conditions, especially soil chemistry for which evidence of cadaver impact was documented for PMIs up to five years (Fancher et al. 2017) although effects may vanish after three years (Anderson et al. 2013). Such differences likely explain differences in community responses among studies and illustrate the need for more studies in different settings. For instance, the colonisation of taxa from nearby non-impacted soils might speed up the recovery whereas priority effects might slow it down.

Microbial "seed bank" and necrophagous hitchhikers

On average, 35% of the CPIs were also found in low abundance at D0 (Fig. 6). It is noteworthy that this proportion remains rather stable (35% ± 3 SD) through the experiment, which could indicate that the contribution of this "seed bank" to the CPIs is independent of the PMI. Part of the soil micro-eukaryotic seed bank is composed of taxa specifically adapted to cadaver disturbance that would stay mostly dormant in non-impacted soils (Lennon and Jones 2011). This strategy is also observed in other highly variable habitats such as vernal pools that dry up during the summer (Sisson et al. 2018). The changes in soils following cadaver decomposition likely induce an increase in the activity and relative abundance of these taxa. However, roughly two thirds of the CPIs were not detected at D0 which would suggest that dispersal from elsewhere (other soils or from the cadaver itself) is an important alternative colonisation strategy. This dispersal can be passive (wind) or mediated by necrophagous animals such as flies, coleoptera, or larger scavengers (Perotti and Braig 2009). Necrophagous hitchhiking is likely to be the most successful strategy given the scattered spatiotemporal distribution of cadaver-impacted soils. These findings are in line with previous results (Metcalf et al. 2016) and suggest the existence of two main strategies for the colonisation of cadaver-impacted soils by microbial eukaryotes: the soil micro-eukaryotic seed bank and dispersal from elsewhere.

Cadaver-associated taxa: a field of mostly unknown diversity

Our results provide evidence that the taxa specific to cadaver-impacted soils are poorly known taxonomically as indicated by the lower PID of CPI in comparison to the CAI (Fig. 7 A). Importantly, the proportion of indicator OTUs having a PID lower than 80% is much higher for CPI than CAI. This is particularly true for the period between 22 and 64 days after the beginning of the experiment (Fig. 7 B). These results highlight an important gap in our knowledge of the soil micro-eukaryotic diversity associated with cadaver-impacted soils. This gap has implications for our understanding of the functional role of soil micro-eukaryotes in the decomposition process and hampers potential use of micro-eukaryotic taxa as bioindicators in a forensic context from a taxonomic perspective.

CONCLUSIONS

Overall, our results confirm that cadaver decomposition constitutes a major disturbance for microbial eukaryotic communities that leads to a transient taxonomic and functional reorganisation of the soil microbial food web. From day 8 to 64, the disturbance induced by cadaver decomposition leads to a reorganisation of communities in favour of bacterivores. Day 64 to 1051 corresponds to a slow recovery of communities where differences to the control soils progressively diminish over time. This period is characterised by an increase in Fungi and a decrease in bacterivores. In addition to these general trends, taxa specific of each decomposition stage were identified. However, the taxonomy and ecology of these taxa remains poorly known suggesting that carcass-impacted soils are unique and very little studied habitats that host a mostly unknown, yet functionally important micro-eukaryotic diversity. Detailed characterization of the ecology and taxonomy of these taxa is critical to further our understanding of the role of microbes in cadaver-impacted soils.

Acknowledgements. This study was funded by the Stiftung Forensisches Forum Frankfurt/Main, Germany; Vereinigung von Freunden und Förderern der Goethe-Universität, Frankfurt/Main, Germany; the University of Neuchâtel, Switzerland; the "Subsides overhead FNS" of the University of Neuchâtel to EM, the Swiss National Science Foundation (project. No 31003A_141188 to E.M. and 31003A_163254 to E.L.), and a SCIEX fellowship to MR (grant no 13.311). MR would like to acknowledge a grant from Switzerland through the Swiss Contribution to the enlarged European Union, Grant: CLIMPEAT (PSPB-013/2010). We thank Dr. Sonia Estelle Tarnawski and Luc Dolivo for preparing the samples for Illumina analysis, Dr. Roxane Kohler-Milleret for infrared spectroscopy and Dr. Emanuela Samaritani for assistance with the Illumina sequencing. B.F and C.V.W.S. acknowledge the WISNA program from the German Federal Ministry of Education and Research. B.F. acknowledges the project "FunShift" (project FO 1420/1-1) awarded by the German Research Foundation.

REFERENCES

Adserias-Garriga J., Hernández M., Quijada N. M., Rodríguez Lázaro D., Steadman D., Garcia-Gil J. (2017) Daily thanatomicrobiome changes in soil as an approach of postmortem interval estimation: An ecological perspective. *Forensic Sci. Int.* **278**: 388–395

Aitkenhead-Peterson J. A., Alexander M. B., Bytheway J. A., Carter D. O., Wescott D. J. (2015) Applications of soil chemistry in forensic entomology. In: J. Tomberlin, M. Benbow (eds.), *Forensic Entomology*, Boca Raton: CRC Press, pp. 283–296 (chapter 23)

Amendt J., Krettek R., Zehner R. (2004) Forensic entomology. *Naturwissenschaften* **91 (2)**: 51–56

Anderson B., Meyer J., Carter D. O. (2013) Dynamics of ninhydrin-reactive nitrogen and pH in gravesoil during the extended postmortem interval. *J. Forensic Sci.* **58 (5)**: 1348–1352

Anderson G. S. (2010) Factors that influence insect succession on carrion. In: J. Byrd, J. Castner (eds.), *Forensic Entomology: The utility of arthropods in legal investigations*, Boca Raton: CRC Press, pp. 201–250

Anthony M. A., Bender S. F., van der Heijden M. G. A. (2023) Enumerating soil biodiversity. *Proc. Natl. Acad. Sci. U.S.A.* **120**: e2304663120

Aoki Y., Hoshino M., Matsubara T. (2007) Silica and testate amoebae in a soil under pine-oak forest. *Geoderma* **142 (1–2)**: 29–35

Barton P. S., Cunningham S. A., Lindenmayer D. B., Manning A. D. (2013) The role of carrion in maintaining biodiversity and ecological processes in terrestrial ecosystems. *Oecologia* **171 (4)**: 761–772

Bass D., Silberman J. D., Brown M. W., Pearce R. A., Tice A. K., Jousset A. et al. (2016) Coprophilic amoebae and flagellates, including *Guttulinopsis*, *Rosculus* and *Helkesimastix*, characterise a divergent and diverse rhizarian radiation and contribute to a large diversity of faecal-associated protists. *Environ. Microbiol.* **18 (5)**: 1604–1619

Belk A. D., Deel H. L., Burcham Z. M., Knight R., Carter D. O., Metcalf J. L. (2018) Animal models for understanding microbial decomposition of human remains. *Drug Discov. Today* **28**: 117–125

Benninger L. A., Carter D. O., Forbes S. L. (2008) The biochemical alteration of soil beneath a decomposing carcass. *Forensic Sci. Int.* **180 (2–3)**: 70–75

Bergmann R. C., Ralebitso-Senior T. K., Thompson T. J. U. (2014) An RNA-based analysis of changes in biodiversity indices in response to *Sus scrofa domesticus* decomposition. *Forensic Sci. Int.* **241**: 190–194

Bouwman L. A., Zwart K. B. (1994) The ecology of bacterivorous protozoans and nematodes in arable soil. *Agr. Ecosyst. Environ.* 145–160

Braig H. R., Perotti M. A. (2009) Carcases and mites. *Exp. Appl. Acarol.* **49**: 45–84

Breton H. A., Kirkwood A. E., Carter D. O., Forbes S.L. (2016) Changes in soil microbial activity following cadaver decomposition during Spring and Summer months in Southern Ontario. In: H. Kars, L. van den Eijkel (eds.), *Soil in Criminal and Environmental Forensics*, Cham: Springer International Publishing, pp. 243–262

Camacho C., Coulouris G., Avagyan V., Ma N., Papadopoulos J., Bealer K., Madden T. L. (2009) BLAST plus: Architecture and applications. *BMC Bioinformatics* **10**: 1–9

Carter D. O., Tibbett M. (2003) *Taphonomic mycota*: Fungi with forensic potential. *J. Forensic. Sci.* **48 (1)**: 168–171

Carter D. O., Yellowlees D., Tibbett M. (2007) Cadaver decomposition in terrestrial ecosystems. *Naturwissenschaften* **94 (1)**: 12–24

Carter D. O., Yellowlees D., Tibbett M. (2010) Moisture can be the dominant environmental parameter governing cadaver decomposition in soil. *Forensic Sci. Int.* **200 (1–3)**: 60–66

Carter D. O., Metcalf J. L., Bibat A., Knight R. (2015) Seasonal variation of postmortem microbial communities. *Forensic Sci. Med. Pathol.* **11**: 202–207

Cobaugh K. L., Schaeffer S. M., DeBruyn J. M. (2015) Functional and structural succession of soil microbial communities below decomposing human cadavers. *PLoS One* **10 (6)**: e0130201

Daria B., Matuszewski S., Konwerski S. (2011) Insect succession on carrion: Seasonality, habitat preference and residency of histerid beetles (Coleoptera: Histeridae) visiting pig carrion exposed in various forests (Western Poland). *Pol. J. Ecol.* **59 (4)**: 787–797

DeBruyn J. M., Hoeland K. M., Taylor L. S., Stevens J. D., Moats M. A., Bandopadhyay S., Dearth S. P., Castro H. F., Hewitt K. K., Campagna S. R., Dautartas A. M., Vidoli G. M., Mundorff A. Z., Steadman D. W. (2021) Comparative decomposition of humans and pigs: Soil biogeochemistry, microbial activity and metabolomic profiles. *Front. Microbiol.* **11**: 2020, art. no. 608856

De Cáceres M., Legendre P. (2009) Associations between species and groups of sites: Indices and statistical inference. *Ecology* **90 (12)**: 3566–3574

Dekeirsschieter J., Verheggen F. J., Gohy M., Hubrecht F., Bourguignon L., Lognay G., Haubruge E. (2009) Cadaveric volatile organic compounds released by decaying pig carcasses (*Sus domesticus L.*) in different biotopes. *Forensic Sci. Int.* **189 (1–3)**: 46–53

Fancher J. P., Aitkenhead-Peterson J. A., Farris T., Mix K., Schwab A. P., Wescott D. J., Hamilton M. D. (2017) An evaluation of soil chemistry in human cadaver decomposition islands: Potential for estimating postmortem interval (PMI). *Forensic Sci. Int.* **279**: 130–139

Ficetola G. F., Canedoli C., Stoch F. (2019) The Racovitzan impediment and the hidden biodiversity of unexplored environments. *Conserv. Biol.* **33**: 214–216

Fiedler S., Kaiser K., Fournier B. (2023) Cadaver imprint on soil chemistry and microbes-knowns, unknowns, and perspectives. *Front. Soil Sci.* **3**: 1107432

Finley S. J., Benbow M. E., Javan G. T. (2015) Microbial communities associated with human decomposition and their potential use as postmortem clocks. *Int. J. Legal Med.* **129**: 623–632

Finley S. J., Pechal J. L., Benbow M. E., Robertson B. K., Javan G. T. (2016) Microbial signatures of cadaver gravesoil during decomposition. *Microb. Ecol.* **71**: 524–529

Forger L. V., Woolf M. S., Simmons T. L., Swall J. L., Singh B. (2019) A eukaryotic community succession based method for postmortem interval (PMI) estimation of decomposing porcine remains. *Forensic Sci. Int.* **302**: 109838

Fu X., Guo J., Finkelbergs D., He J., Zha L., Guo Y., Cai J. (2019) Fungal succession during mammalian cadaver decomposition and potential forensic implications. *Sci. Rep.* **9**: 12907

García-Rojo A. M., Martínez-Sánchez A., López R., de la Vega J. M. G., Rica M., González M., Disney R. H. L. (2013) A mathematical model applied for assisting the estimation of PMI in a case of forensic importance. First record of *Conicera*

similis (Diptera: Phoridae) in a corpse. *Forensic Sci. Int.* **231 (1–3)**: e11–e18

Geisen S., Mitchell E. A. D., Adl S., Bonkowski M., Dunthorn M., Ekelund F. et al. (2018) Soil protists: A fertile frontier in soil biology research. *FEMS Microbiol. Rev.* **42 (3)**: 293–323

Geisen S., Lara E., Mitchell E. A. D., Völcker E., Krashevska V. (2020) Soil protist life matters! *Soil Org.* **92 (3)**: 189–196

Guillou L., Bachar D., Audic S., Bass D., Berney C., Bittner L. et al. (2013) The protist ribosomal reference database (PR^2): A catalog of unicellular eukaryote Small Sub-Unit rRNA sequences with curated taxonomy. *Nucleic Acids Res.* **41 (1)**: D597–D604

Hanski I. (1987) Carrion fly community dynamics: Patchiness, seasonality and coexistence. *Ecol. Entomol.* **12 (3)**: 257–266

Houston D. C. (1985) Evolutionary ecology of afrotropical and neotropical vultures in forests. *Ornithol. Monogr.* **(36)**: 856–864

Kuhn M. (2020) caret: Classification and Regression Training. URL https://CRAN. R-project.org/package=caret. R package version 6.0–86

Külling N., Adde A., Fopp F., Schweiger A. K., Broeznimann O., Rey P.-L., Giuliani G., Goicolea T., Petitpierre B., Zimmermann N. E., Pellissier L., Altermatt F., Lehmann A., Guisan A. (2024). SWECO25: A cross-thematic raster database for ecological research in Switzerland. *Scientific Data* **11 (1)**: 21. https://doi.org/10.1038/s41597-023-02899-1

Lauber C. L., Metcalf J. L., Keepers K., Ackermann G., Carter D. O., Knight R. (2014) Vertebrate decomposition is accelerated by soil microbes. *Appl. Environ. Microbiol.* **80 (16)**: 4920–4929

Lax G., Eglit Y., Eme L., Bertrand E. M., Roger A. J., Simpson A. G. B. (2018) Hemimastigophora is a novel supra-kingdom-level lineage of eukaryotes. *Nature* **564 (7736)**: 410–414

Lefebvre F., Gaudry E. (2009). Forensic entomology: A new hypothesis for the chronological succession pattern of necrophagous insect on human corpses. *Ann. Soc. entomol. Fr.*, vol. 45, Taylor & Francis, pp. 377–392

Lennon J. T., Jones S. E. (2011) Microbial seed banks: The ecological and evolutionary implications of dormancy. *Nat. Rev. Microbiol.* **9 (2)**: 119–130

Lentendu G., Singer D., Agatha S., Bahram M., Hannula S. E., Helder J., Tedersoo L., Traunspurger W., Geisen S., Lara E. (2025) A holistic eukaryotic functional reference for automated profiling of soil Eukaryotes. Mol. Ecol. Resour., **n/a**, e14118.

Mahé F., Rognes T., Quince C., de Vargas C., Dunthorn M. (2015) Swarm v2: highly-scalable and high-resolution amplicon clustering. PeerJ 3: e1420

Martin M. (2011) Cutadapt removes adapter sequences from high-throughput sequencing reads. *EMBnet J* **17 (1)**: 10–12

Masella A. P., Bartram A. K., Truszkowski J. M., Brown D. G., Neufeld J. D. (2012) PANDAseq: Paired-end assembler for illumina sequences. *BMC Bioinformatics* **13**: 1–7

Mason A. R., Taylor L. S., DeBruyn J. M. (2023) Microbial ecology of vertebrate decomposition in terrestrial ecosystems. *FEMS Microbiol. Ecol.* **99**: fiad006

Metcalf J. L., Xu Z. Z., Weiss S., Lax S., Van Treuren W., Hyde E. R. et al. (2016) Microbial community assembly and metabolic function during mammalian corpse decomposition. *Science* **351 (6269)**: 158–162

Mikhailov K. V., Tikhonenkov D. V., Janouškovec J., Diakin A. Y., Ofitserov M. V., Mylnikov A. P., Aleshin V. V. (2015) Primary structure of 28S rRNA gene confirms monophyly of free-living heterotrophic and phototrophic apicomplexans (Alveolata). *Biochemistry* **80**: 1492–1499

Moreno L. I., Mills D., Fetscher J., John-Williams K., Meadows-Jantz L., McCord B. (2011) The application of amplicon length heterogeneity PCR (LH-PCR) for monitoring the dynamics of soil microbial communities associated with cadaver decomposition. *J. Microbiol. Methods* **84**: 388–393

Palarea-Albaladejo J., Martin-Fernandez J. A. (2015) zCompositions – R package for multivariate imputation of left-censored data under a compositional approach. **143**: 85–96. URL http://dx.doi.org/10.1016/j.chemolab.2015.02.019

Parkinson R. A., Dias K., Horswell J., Greenwood P., Banning N., Tibbett M., Vass A. A. (2009) Microbial community analysis of human decomposition on soil. In: K. Ritz, L. Dawson, D. Miller (eds.), *Criminal and Environmental Soil Forensics*, Springer, pp. 379–394

Pawlett M., Rickson R. J., Niziolomski J., Churchill S., Kešner M. (2019) Human cadaver burial depth affects soil microbial and nutrient status. *Forensic Archaeology Anthropol. Ecol.* **1 (2)**: 119–125

Payne J. A. (1965) A summer carrion study of the baby pig *Sus scrofa* Linnaeus. *Ecology* **46 (5)**: 592–602

Perotti M. A., Braig H. R. (2009) Phoretic mites associated with animal and human decomposition. *Exp. Appl. Acarol.* **49**: 85–124

Rognes T., Flouri T., Nichols B., Quince C., Mahé F. (2016) VSEARCH: A versatile open source tool for metagenomics. PeerJ 4

Schloss P. D., Westcott S. L., Ryabin T., Hall J. R., Hartmann M., Hollister E. B. et al. (2009) Introducing mothur: Open-source, platform-independent, community-supported software for describing and comparing microbial communities. *Appl. Environ. Microbiol.* **75 (23)**: 7537–7541

Schroter D., Wolters V., De Ruiter P. C. (2003) C and N mineralisation in the decomposer food webs of a European forest transect. *Oikos* **102 (2)**: 294–308

Seppey C. V. W., Fournier B., Szelecz I., Singer D., Mitchell E. A. D., Lara E. (2016) Response of soil euglyphid testate amoebae (Rhizaria: Cercozoa) to pig cadavers assessed by high-throughput sequencing. *Int. J. Legal. Med.* **130 (2)**: 551–562

Singer D., Seppey C. V. W., Lentendu G., Dunthorn M., Bass D., Belbahri L., Blandenier Q., Debroas D., de Groot G. A., de Vargas C., Domaizon I., Duckert C., Izaguirre I., Koenig I., Mataloni G., Schiaffino M. R., Mitchell E. A. D., Geisen S., Lara E. (2021) Protist taxonomic and functional diversity in soil, freshwater and marine ecosystems. *Environ. Int.* **146**: 106262

Sisson C., Gulla-Devaney B., Katz L. A., Grattepanche J.-D. (2018) Seed bank and seasonal patterns of the eukaryotic SAR (Stramenopila, Alveolata and Rhizaria) clade in a New England vernal pool. *J. Plankton Res.* **40**: 376–390

Stokes K. L., Forbes S. L., Benninger L. A., Carter D. O., Tibbett M. (2009) Decomposition studies using animal models in contrasting environments: evidence from temporal changes in soil chemistry and microbial activity. In: K. Ritz, L. Dawson, D. Miller (eds.) *Criminal and Environmental Soil Forensics*, Springer, pp. 357–377

Stokes K. L., Forbes S. L., Tibbett M. (2013) Human versus animal: Contrasting decomposition dynamics of mammalian analogues in experimental taphonomy. *J. Forensic Sci.* **58 (3)**: 583–591

Szelecz I., Fournier B., Seppey C. V. W., Amendt J., Mitchell E. A. D. (2014) Can soil testate amoebae be used for estimating the time since death? A field experiment in a deciduous forest. *Forensic Sci. Int.* **236**: 90–98

Szelecz I., Sorge F., Seppey C. V. W., Mulot M., Steel H., Neilson R. et al. (2016) Effects of decomposing cadavers on soil

nematode communities over a one-year period. *Soil Biol. Biochem.* **103**: 405–416

Szelecz I., Lösch S., Seppey C. V. W., Lara E., Singer D., Sorge F. et al. (2018) Comparative analysis of bones, mites, soil chemistry, nematodes and soil micro-eukaryotes from a suspected homicide to estimate the post-mortem interval. *Sci. Rep. UK* **8 (1)**: 25

Tibbett M., Carter D. O. (2009) Research in forensic taphonomy: A soil-based perspective. In: K. Ritz, L. Dawson, D. Miller (eds.), *Criminal and Environmental Soil Forensics*, Springer, pp. 317–331

Turchetto M., Lafisca S., Costantini G. (2001) Postmortem interval (PMI) determined by study sarcophagous biocenoses: Three cases from the province of Venice (Italy). *Forensic Sci. Int.* **120 (1–2)**: 28–31

Wang Y., Wang M., Luo C., Li L., Xu W., Hu G., Wang Y., Amendt J., Wang J. (2021) Dynamics of insects, microorganisms and muscle mRNA on pig carcasses and their significances in estimating PMI. *Forensic Sci. Int.* **329**: 111090

Wilkinson D. M., Mitchell E. A. D. (2010) Testate amoebae and nutrient cycling with particular reference to soils. *Geomicrobiol. J.* **27 (6–7)**: 520–533

Worley A. C., Raper K. B., Hohl M. (1979) *Fonticula alba* – New cellular slime-mold (Acrasiomycetes). *Mycologia* **71 (4)**: 746–760

Received on 29th November, 2024; revised on 15th April, 2025; accepted on 27th May, 2025

Supplementary Material

Table S1. Relative abundance of 1916 indicator OTUs at days 8, 15, 22, 33, 64, 300 and 1051, in the three replicates of the Control (C), Fake pig (F) and Pig cadaver (P) plots with indication of the p-Value of the IndVal analysis and taxonomic assignment from the PR^2 database.

Fig. S1. Taxonomy assigned to the overall OTU found below carcass un-impacted (tCA) and impacted (tCP) soils. The proportions are calculated on the relative abundance of each OTU in each sample.

Fig. S2. Relationship between the postmortem interval (PMI) and the calculated accumulated degree days.

Fig. S3. Amount of carbon (C), nitrogen (N) and C/N ratio in soils impacted by cadaver (green), fake cadaver (red) and control (black). The grey bars represent standard error

Fig. S4. Taxonomic proportions of micro-eukaryotes through time. The number above the pie charts indicate the PMI.

Fig. S5. Redundancy analysis calculated on the protist communities retrieved from soil impacted fake cadaver (red) and control (black). The arrows show the change in community through PMI and the black dot show the initial communities.

Fig. S6. Bioindicators OTUs of a given PMI (one to seven samplings in a row) for communities found under decomposing pigs. Black, red and green lines represent the control, fake pig and cadaver treatments respectively. The grey bars represent the standard error for each sampling and treatment.

Fig. S7. Density distribution of soil micro-eukaryotic indicator OTUs of carcass absence (blue) or presence (green) in function of their abundance in their respective dataset (transformed by centred log ratio: CLR). The black boxes show the 1st and 3rd quartiles of the distribution while the vertical line indicates the median of the distribution. As the sum of the CLR transformed dataset in each sample is 0, it is normal to have OTUs with a CLR sum below 0. The barplots on the top right corner indicate the proportion of the overall soil protist diversity corresponding to the carcass absence (CAI, blue) and presence (CAP, green) indicators.

Fig. S8. Difference in the NMDS coordinates (from Fig. 3) between protist OTUs communities of a given PMI and the initial sampling (grey) or the control of the given PMI (black). All differences were calculated within blocks.

Fig. S9. Taxonomic proportions of carcass absence indicators through time within the cadaver un-impacted plots. The number above the pie charts indicate the PMI. The pie of Day0 indicates the relative abundance of carcass indicators found at D0. Organisms belonging to underrepresented clades at taxonomic level 2 are pooled into the category “rare_tax_lev_2”.